Available online at www.sciencedirect.com

ScienceDirect

www.elsevier.com/locate/jes

JES JOURNAL OF ENVIRONMENTAL SCIENCES

www.jesc.ac.cn

# Disinfection byproducts and halogen-specific total organic halogen speciation in chlorinated source waters – The impact of iopamidol and bromide

*Nana Osei B. Ackerson* [1], *Hannah K. Liberatore* [2], *Michael J. Plewa* [3], *Susan D. Richardson* [2], *Thomas A. Ternes* [4], *Stephen E. Duirk* [1,*]

[1] *Department of Civil Engineering, University of Akron, Akron, OH 44325, USA*
[2] *Department of Chemistry and Biochemistry, University of South Carolina, Columbia, SC 29208, USA*
[3] *Department of Crop Sciences and Safe Global Water Institute, University of Illinois at Urbana-Champaign, Urbana, IL 61801, USA*
[4] *Federal Institute of Hydrology (BfG), D-56068 Koblenz, Germany*

ARTICLE INFO

*Article history:*
Received 6 August 2019
Received in revised form
19 October 2019
Accepted 21 October 2019
Available online 8 November 2019

*Keywords:*
Iopamidol
Total organic halogen (TOX)
Disinfection byproducts (DBPs)
Chlorine
Natural organic matter (NOM)
pH

ABSTRACT

This study investigated the speciation of halogen-specific total organic halogen and disinfection byproducts (DBPs) upon chlorination of natural organic matter (NOM) in the presence of iopamidol and bromide ($Br^-$). Experiments were conducted with low bromide source waters with different NOM characteristics from Northeast Ohio, USA and varied spiked levels of bromide (2–30 μmol/L) and iopamidol (1–5 μmol/L). Iopamidol was found to be a direct precursor to trihalomethane (THM) and haloacetic acid formation, and in the presence of $Br^-$ favored brominated analogs. The concentration and speciation of DBPs formed were impacted by iopamidol and bromide concentrations, as well as the presence of NOM. As iopamidol increased the concentration of iodinated DBPs (iodo-DBPs) and THMs increased. However, as $Br^-$ concentrations increased, the concentrations of non-brominated iodo- and chloro-DBPs decreased while brominated-DBPs increased. Regardless of the concentration of either iopamidol or bromide, bromochloroiodomethane (CHBrClI) was the most predominant iodo-DBP formed except at the lowest bromide concentration studied. At relevant concentrations of iopamidol (1 μmol/L) and bromide (2 μmol/L), significant quantities of highly toxic iodinated and brominated DBPs were formed. However, the rapid oxidation and incorporation of bromide appear to inhibit iodo-DBP formation under conditions relevant to drinking water treatment.



* *Corresponding author.*
E-mail address: duirk@uakron.edu (S.E. Duirk).

https://doi.org/10.1016/j.jes.2019.10.007
1001-0742/

## Introduction

The formation and speciation of disinfection byproducts (DBPs) is highly dependent on source water characteristics and in-plant treatment processes. Source water characteristics mostly found to influence DBP formation are concentration of DBP precursors, type and concentration of disinfectant, and aqueous conditions like pH (Hu et al., 2010). Natural organic matter (NOM) has been studied extensively as a DBP precursor since chlorination of water containing NOM results in the formation of chlorinated DBPs (chloro-DBPs) like chloroform ($CHCl_3$) and trichloroacetic acid (TCAA) (Duirk and Valentine, 2007; Hua et al., 2015). However, if the source water contains bromide ($Br^-$), aqueous chlorine oxidizes the bromide to hypobromous acid (HOBr), which is in equilibrium (i.e., $pK_a$ = 8.8) with hypobromite ion ($OBr^-$) (Kumar and Margerum, 1987). HOBr incorporates more readily than HOCl into NOM to form brominated DBPs (bromo-DBPs) (Hua et al., 2006; Criquet et al., 2015). Increasing concentrations of $Br^-$ produces mixed halogenated DBPs to fully brominated DBPs (Cowman and Singer, 1996; Hua et al., 2006).

The presence of iodide ($I^-$) in source water also affects DBP speciation during disinfection. Aqueous chlorine oxidizes $I^-$ to hypoiodous acid (HOI) (Nagy et al., 1988). HOI, just like HOBr, incorporates more readily into NOM to form iodinated DBPs (iodo-DBPs) or can further be oxidized to iodate ($IO_3^-$) in the presence of excess chlorine (Bichsel and von Gunten, 1999). Iodo-DBPs have attracted attention because they are more genotoxic and cytotoxic than the other halogenated analogs (Plewa et al., 2004, 2010; Richardson et al., 2008; Wagner and Plewa, 2017). Studies revealed that iodoform ($CHI_3$) and iodoacetic acid (IAA) illicit higher cytotoxicity and genotoxicity than their brominated/chlorinated analogs (Duirk et al., 2011; Wagner and Plewa, 2017). Iodoacetic acid (IAA) is also tumorigenic in mice (Wei et al., 2013) and the mechanism for IAA genotoxicity was determined (Attene-Ramos et al., 2010; Dad et al., 2013; Pals et al., 2013). Iodide in source water can be from seawater intrusion, seawater desalination, or fossilized seawater (Hua et al., 2006; Agus et al., 2009). Also, studies demonstrated that some iodinated X-ray contrast media (ICM) (Ackerson et al., 2018; Wendel et al., 2014; Duirk et al., 2011; Postigo et al., 2018) and thyroxine (Duan et al., 2016) are precursors to iodo-DBP formation.

ICM are pharmaceuticals used to enhance visualization of internal organs and other soft tissue (Christiansen, 2005). Their structures consist of iodine substituted at the 2, 4, and 6 positions of a benzene ring as the base structure, with side chains comprised of amide and hydroxyl moieties, which make ICM extremely soluble in water (Krause and Schneider, 2002). ICM have been detected in wastewater effluents, creeks, rivers, and source waters at ng/L to high μg/L concentrations (Ternes and Hirsch, 2000; Seitz et al., 2006; Duirk et al., 2011; Watanabe et al., 2016). Based on a 2011 study of 10 U.S. drinking water treatment plants, the most commonly detected ICM in source waters was iopamidol (found in 6/10 plants sampled), with iohexol (3/10 plants), iopromide (3/10 plants), and diatrizoate (1/10 plants) also detected (Duirk et al., 2011). These ICM are not toxic, but when released into drinking water sources, can be transformed during disinfection processes to produce iodine-containing DBPs (Wendel et al., 2014; Zhao et al., 2014; Matsushita et al., 2015; Tian et al., 2017). Advanced oxidation processes can also transform ICM. For example, titanium dioxide ($TiO_2$) photolytic oxidation of iomeprol showed a fast transformation of iomeprol and simultaneous increase in iodide (Doll and Frimmel, 2005). Furthermore, Zhao et al. (2014) found that iopamidol was transformed in Fe(III)-oxalate/$H_2O_2$ photochemical system using ultraviolet (UV) and visible light irradiation to form different high molecular weight iopamidol DBPs. Also, enhanced transformation of diatrizoate with UV/$S_2O_8^{2-}$ was found in a photochemical process (Duan et al., 2016). Using $H_2O_2$ and $S_2O_8^{2-}$ activated with zero valent aluminum to treat iopamidol, Arslan-Alaton et al. (2016) achieved up to 41% iopamidol removal in surface water and treated sewage. However, iopamidol is the only commonly detected ICM known to exhibit significant reactivity with aqueous chlorine to form both high- and low-molecular weight DBPs (Duirk et al., 2011; Wendel et al., 2014; Matsushita et al., 2015). In a different chlorination study, Ye et al. (2014) observed that iopamidol produced exceedingly higher yields of iodo-THMs than other ICM (histodenz, iodixanol, diatrizoate, and iopromide) in the presence of NOM.

The overall objective of this study was to investigate the formation and speciation of halogen-specific total organic halogen (TOX) and DBPs as a function of iopamidol and bromide concentrations. Since iodo-DBP formation is slow due to iopamidol transformation into products that participate in iodide exchange (Wendel et al., 2014), rapid oxidation and incorporation of bromide into DBP precursors may inhibit iodo-DBP formation. Two source waters with different NOM characteristics were chlorinated in the presence of varying concentrations of iopamidol and bromide. Halogen specific TOX and DBPs were measured after 48 hr to investigate how iopamidol/bromide DBP precursors either enhance or suppress the formation of cytotoxic and genotoxic DBPs, as precursor transformation and NOM incorporation rate could impact the resulting toxicity of finished water disinfected with aqueous chlorine.

## 1. Materials and methods

### 1.1. Standards and reagents

Reagents of highest available purity were used for all analyses. Additional information on standards used are described in Appendix A. All stock solutions were prepared with purified water (18.2 MΩ/cm) from Barnstead ROPure Infinity/NANOPure system (Barnstead-Thermolyne Corp. Dubuque, IA, USA).

### 1.2. Source water characterization

Two source waters (SWs) from the Barberton drinking water treatment plant (WTP) (Barberton, OH, USA), and Garret Morgan WTP (Cleveland, OH, USA), were used in this study. These SWs were selected due to their different NOM characteristics and concentrations. The differences in NOM characteristics have been observed to influence their reactivity with chlorinated oxidants (Ackerson et al., 2018). The characteristics of

the SWs (Appendix A; Table S1) and the fluorescence spectra were described previously (Ackerson et al., 2018).

### 1.3. Experimental procedures

Aqueous chlorine was prepared monthly from 5.8% to 6% sodium hypochlorite (Thermo Fisher Scientific, Pittsburgh, PA), which contained equimolar amounts of $OCl^-$ and $Cl^-$. The molar concentrations of $OCl^-$ and $Cl^-$ were verified using method described by Duirk et al. (2006). Prior to each experiment, the concentration of aqueous chlorine was determined with ferrous ammonium sulfate (FAS)/N, N′-diphenyl-p-phenylenediamine (DPD) titration (APHA et al., 2005). All glassware and polytetrafluoroethylene (PTFE) were soaked in a chlorine bath for 24 hr, rinsed with copious amount of purified water, and dried before use. The pH for each experiment was monitored with an Orion 5-star pH meter equipped with Ross ultra-combination electrode (Thermo Fisher Scientific, Pittsburgh, PA). Both phosphate (for pH 6.5 and 7.5) and borate (for pH 8.5 and 9.0) buffer solutions were used to maintain pH while 1 N $H_2SO_4$ and 1 N NaOH were used to adjust pH in each reactor. The concentrations of the buffer solutions for TOX and DBP experiments were 1.0 and 4.0 mM respectively. Lower buffer concentration was used in TOX studies to mitigate the excessively large peaks interferences in the ion chromatogram.

Experiments were conducted using either purified water or SW. Chlorination experiments in purified water were spiked with iopamidol and bromide resulting in concentrations of 5.0 μmol/L and 15 μmol/L, respectively. Experiments were either conducted in 250 mL or 1000 mL Erlenmeyer flasks at pH 6.5–9.0. The 250-mL reactors were used for TOX, iodate, bromate, and halide experiments while the 1000-mL reactors were used for DBP quantification. About 100 μmol/L aqueous chlorine was added to the reaction mixture under rapid mix conditions. Aliquots of the samples were transferred into 128 mL amber bottles and 40 mL amber vials capped headspace free with PTFE-lined caps and incubated in the dark at 25 ± 1°C for 0–72 hr. At the end of the reaction time, the residual chlorine in the amber bottles was quenched with a sulfite solution, 20% molar excess of the initial oxidant concentration and extracted immediately for DBP analysis. Samples in 40 mL amber vials were split into aliquots of 5 mL for iodate and halide analysis and 30 mL for TOX analysis. Residual chlorine in samples for iodate and TOX/halide was quenched with 120 μmol/L resorcinol and sulfite solutions, respectively, as described previously (Ackerson et al., 2018). Resorcinol was used for iodate samples because sulfite can reduce $IO_3^-$ to $I^-$ (Rabai et al., 1987).

Chlorination experiments using Barberton source water (BSW) and Cleveland source water (CSW) were conducted to address the impact of bromide and iopamidol, separately, on DBP formation. First, batch reactors (1000 mL or 250 mL Erlenmeyer flasks) were filled with SWs dosed with 5 μmol/L iopamidol and $Br^-$ concentrations were varied from 2.0 to 30 μmol/L at pH 6.5–9.0. Aqueous chlorine (100 μmol/L) was added to the rapidly mixed sample. Using the same protocol above aliquots of the samples were stored headspace free at 25 ± 1°C for 0–48 hr, after which residual chlorine was quenched. Secondly, using the same experimental protocol, bromide concentration was maintained at 15 μmol/L, while iopamidol concentrations were varied at 1.0–5.0 μmol/L. After quenching residual chlorine, samples were prepared for TOX, iodate, halide, and DBP analysis. All chlorination experiments in SWs were performed in duplicates or triplicates and the average data were presented. However single experiments were performed for chlorination of purified water.

### 1.4. Analytical procedures

Water samples (30 mL) for TOX analysis were acidified with 70% nitric acid to < pH 2, concentrated on pre-packed granular activated carbons, inorganic halides rinsed with 15 mL $KNO_3$ solution, combusted in a TOX-100 analyzer (Cosa Instruments/Mitsubishi, Horseblock Road, NY), and the off-gas (hydrogen halides) was absorbed into a 20 mL phosphate solution (100 μmol/L). Thus, total organic bromine (TOBr), total organic chlorine (TOCl) and total organic iodine (TOI) were detected respectively as $Br^-$, $Cl^-$, and $I^-$ using ion chromatography (Dionex ICS-3000, Dionex Corporation, Sunnyvale, CA, with a conductivity detector and an ASRS®300 4 mm anion self-regenerating suppressor). The limit of detection for each TOX was 0.5 μmol/L. Quenched samples for iodate and halide analysis were analyzed in treated waters and source waters, respectively, without further treatment, using ion chromatography. Iodate was detected with an AS18 analytical column, while detection of halides was achieved with an AS20 analytical column (4 × 250 mm) and guard column (Dionex Corporation, Sunnyvale, CA) with 10 mmol/L KOH eluent (1 mL/min).

Trihalomethanes (THMs), haloacetic acids (HAAs), and haloacetonitriles (HANs) were the classes of DBPs analyzed. The list of THMs, HANs, and HAAs analyzed are shown in Appendix A Table S2. Samples for DBPs were acidified to pH 1 using concentrated sulfuric acid and extracted using methyl *tert*-butyl ether (MtBE). 1,2-Dibromopropane was used as the internal standard. The organic extract was split into two aliquots: 1.5 mL was used for THM and HAN analysis, while 0.5 mL was derivatized with diazomethane for HAA analysis. The extraction and derivatization procedures are found in Ackerson et al. (2018). THMs, HANs, and HAAs (except iodo-HAAs) were analyzed with a 7890A gas chromatography (GC) system equipped with $^{63}Ni$ microelectron capture detector (μECD) (Agilent Technologies, Santa Clara, CA). Samples were injected onto an Rxi-5Sil MS (30 m × 0.25 mm i.d., 0.25 μm film thickness, Restek Corporation, Bellefonte, PA) GC column using splitless injection. The make-up and carrier gases were ultrahigh purity nitrogen and helium gases respectively. The μECD temperature was 250°C. The temperature program for THM and HAN detection is described by Ackerson et al. (2018). The temperature program for the separation of HAAs was 50°C initial temperature for 10 min, 0.35°C/min to 66°C and held for 5 min, 6°C/min to 150°C and held for 5 min, 20°C/min to 210°C and held for 3 min and finally 35°C/min to 280°C. Iodo-HAAs were analyzed using GC-MS/MS with a Thermo-Scientific Quantum GC- triple quadrupole mass spectrometer coupled to a TRACE GC Ultra gas chromatograph (Thermo-Scientific, Waltham, MA). Detailed analytical procedures are described in previous studies (Allen et al., 2017; Ackerson et al., 2018; Postigo et al., 2018).

## 2. Results and discussion

### 2.1. TOX and DBP formation in the absence of NOM

Previous work has shown that chlorination of iopamidol without NOM present results in an array of DBPs. The transformation of iopamidol by aqueous chlorine results in the formation of TOCl, TOI, iodate, $CHCl_3$, dichloroiodomethane ($CHCl_2I$), and TCAA (Wendel et al., 2014; Ackerson et al., 2018). Therefore, the addition of bromide was expected to result in the formation of brominated DBPs, as well as other mixed bromo/chloro/iodo-DBPs. To understand the potential impact of bromide, an experiment was conducted at pH 6.5, 7.5, 8.5, and 9 in purified water dosed with 5.0 μmol/L iopamidol (i.e., $[TOI]_o$ = 15 μmol/L), 15 μmol/L $Br^-$, and 100 μmol/L aqueous chlorine. At the end of 72 hr, approximately 45%–55% and 44%–53% of the iodine species were TOI and iodate, respectively. Iodine mass balance was achieved through TOI and iodate measurements, as the summed concentration of TOI and iodate accounted for 99.7%–104.8% of the $[TOI]_o$, except at pH 8.5. At pH 8.5, 10% of the $[TOI]_o$ was unaccounted for by TOI and iodate measurements, which could be attributed to incomplete recovery (adsorption) on the activated carbon used in the TOX method. In $Br^-$ spiked reactors, TOI loss and subsequent iodate formation were lower than in reactors without $Br^-$ (Ackerson et al., 2018). Since HOBr reacts/incorporates faster than HOCl and HOI, it may have reacted with iopamidol DBPs on the amide side chain (Heeb et al., 2014) increasing steric hinderance. This may have decreased deiodination which limited iodate formation and TOI loss. Neither TOI nor iodate exhibited any discernible pH pattern.

TOCl formation was between 7 and 9 μmol/L over the entire pH range, while 63%–84% of bromide was incorporated to produce TOBr (9.3–12.6 μmol/L). Generally, the formation of TOBr and TOCl increased with increasing pH. In sample aliquots quenched with resorcinol for inorganic halogen analyses, $Br^-$ was detected at 1.6–4.7 μmol/L, while bromate was below the limit of detection (0.5 μmol/L). Total bromine mass balances based on the sum of TOBr and $Br^-$ concentrations compared to the initial spiked concentration of $Br^-$ (15 μmol/L) were 94%, 96%, 99%, and 95% at pH 6.5, 7.5, 8.5, and 9.0, respectively.

Formations of TOI and iodate were due to the degradation of iopamidol initiated by the nucleophilic attack of $OCl^-$ on one of the amide side chains of iopamidol to form DBPs (Duirk et al., 2011). Subsequent electrophilic oxidation reactions resulted in the release of iodine from iopamidol DBPs to form of HOI (Nagy et al., 1988; Troy et al., 1991), which is further oxidized to iodate by chlorine/bromine oxidants (Bichsel and von Gunten, 1999; Criquet et al., 2012). With iopamidol degradation occurring relatively quickly (i.e., less than 24 hr), iopamidol DBPs still contributed to TOI quantities (Wendel et al., 2014; Matsushita et al., 2015) with small contributions to TOI from lower molecular weight iodo-DBPs (e.g., iodo-THMs and IAAs). TOBr formation can be attributed to the non-selective incorporation of bromine into iopamidol and lower molecular weight DBPs.

Under the experimental conditions, identifiable bromo/chloro/iodo-DBPs were formed as well. The only THMs formed at the end of 72 hr were $CHCl_3$, bromodichloromethane ($CHBrCl_2$), dibromochloromethane ($CHBr_2Cl$), bromoform ($CHBr_3$), and bromochloroiodomethane (CHBrClI) (Fig. 1b). In comparison to a previous study (Ackerson et al., 2018), $CHCl_3$ quantities were suppressed (97%–99%) by the presence of $Br^-$, which was due to the formation of bromo-THMs. $CHCl_3$ and $CHBr_3$ increased with pH except at pH 9.0 where there was a marginal drop in the concentration of $CHCl_3$. CHBrClI was the predominant THM formed, and there was no observation of $CHCl_2I$. The only HAA detected was TCAA (Fig. 1b). Also, the TCAA concentration in the presence of $Br^-$ relative to its concentration in the absence of $Br^-$ decreased by 99%. TCAA concentrations decreased with increasing pH. The presence of $Br^-$ inhibited the formation of $CHCl_2I$ which was detected in the absence of $Br^-$. However, as expected, the presence of $Br^-$ significantly shifted the speciation of DBPs and TOX, as well as observed molar concentrations compared to the absence of bromide.

### 2.2. Formation of TOX and DBP at different iopamidol concentration in the presence of NOM

TOX and DBP formation was then examined in chlorinated source waters where both bromide and iopamidol were added. The two source waters, BSW and CSW, were dosed with bromide (15 μmol/L) and iopamidol (1.0–5.0 μmol/L) prior to the

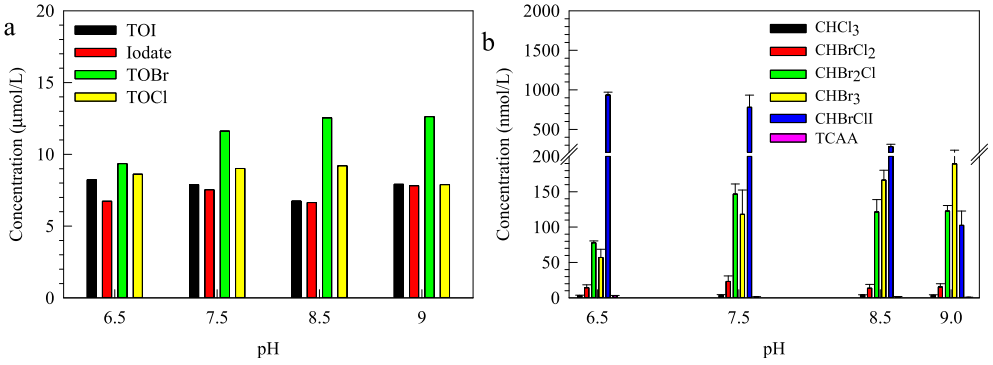


**Fig. 1 – Formation of TOX, iodate and DBPs at 72 hr in chlorinated reaction mixture containing iopamidol and bromide as a function of pH. $[Cl_2]_T$ = 100 μmol/L, $[Br^-]$ = 15 μmol/L, [Iopamidol] = 5.0 μmol/L, $[Buffer]_{TOX}$ = 1.0 mmol/L, $[Buffer]_{DBP}$ = 4.0 mmol/L, and temperature = 25°C.**

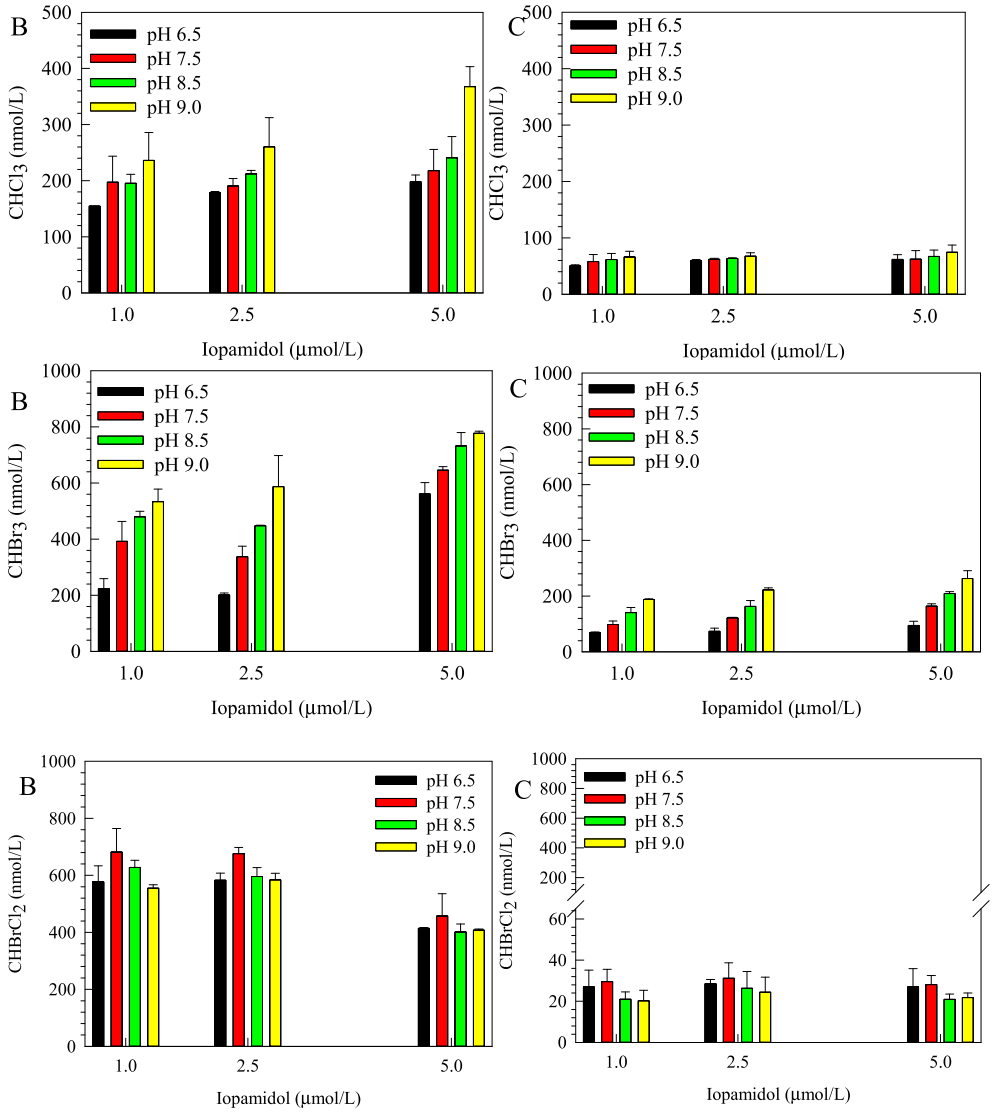


**Fig. 2 – $CHCl_3$, $CHBr_3$, and $CHBrCl_2$ formation in chlorinated Barberton (B) and Cleveland (C) source waters as a function of iopamidol concentration and pH. $[Cl_2]_T = 100$ μmol/L, [Iopamidol] = 1.0–5.0 μmol/L, $[Br^-] = 15$ μmol/L, $[Buffer]_T = 4$ mmol/L, Temp = 25C, $DOC_{Barberton} = 4.47$ mg/L-C, $DOC_{Cleveland} = 2.51$ mg/L-C. Error bars represent 95% confidence interval for two replicates.**

addition of aqueous chlorine (100 μmol/L). Appendix A Fig. S1 shows that the percentage of TOI loss was between 15% and 30% in the SWs at the end of 48-hr chlorine exposure regardless of iopamidol concentration, and the residual TOI concentration in BSW was higher than CSW. This could be due to the higher DOC concentration and $SUVA_{254}$ in BSW and higher reactivity with aqueous chlorine than CSW. Therefore, a lower reactivity of aqueous chlorine with CSW allowed greater reactions with iopamidol, increasing transformation to iopamidol DBPs and enhanced HOI formation. However, no inorganic iodine species ($I^-$ or $IO_3^-$) were detected from the reaction of HOI with active oxidants present. This could be due to incomplete recovery during adsorption on the activated carbon during the TOX extraction. Most of the bromide was incorporated into either NOM or iopamidol DBPs to form TOBr in BSW. Nonetheless, between 75 and 93% bromine incorporation was detected in CSW as TOBr (Appendix A Fig. S1). TOBr formation showed no dependence on iopamidol concentrations, which could be a result of the rapid oxidation of bromide to HOBr and incorporation into either NOM (Westerhoff et al., 2004) or iopamidol DBPs. In addition, at pH 6.5 to 9.0, about 8%–12% of chlorine was incorporated, resulting in TOCl formation (Appendix A Fig. S1). The higher concentrations of TOCl detected in CSW versus BSW could be due to aqueous chlorine preferentially reacting with iopamidol DBPs because of the low reactivity of CSW NOM.

The presence of iopamidol and bromide showed significant differences in DBP formation and speciation compared to the absence of bromide. Generally, the formation of the DBPs may have been influenced by both iopamidol and NOM. However, as expected substantial contributions may come from NOM due to its reactive sites with the oxidants (hypohalous acids (HOX)) (Christman et al., 1983). $CHCl_3$ increased with increasing iopamidol concentration, with higher

concentrations detected in BSW than CSW (Fig. 2). With respect to each pH, $CHBr_3$ increased with increasing iopamidol concentration (Fig. 2). From 1.0 to 2.5 μmol/L iopamidol, $CHBr_3$ increased by <10% in BSW and 8%–25% in CSW. However, a significant increase was observed in BSW when iopamidol increased from 2.5 to 5.0 μmol/L. Both $CHCl_3$ and $CHBr_3$ increased with iopamidol because iopamidol contributed to the formation of these species without NOM, and this may have contributed to the levels observed in addition to the possible substantial contribution from NOM. Almost equal concentrations of $CHBrCl_2$ (570–690 nmol/L) were formed at iopamidol concentrations of 1.0 and 2.5 μmol/L, but decreased to almost 450 nmol/L at 5.0 μmol/L in BSW (Fig. 2). Nearly equal concentrations of $CHBrCl_2$ (20–31 nmol/L) were formed in CSW at all iopamidol concentrations. While more $CHBr_2Cl$ was formed in the BSW (850-1300 nmol/L) than CSW, neither SW displayed any recognizable DBP formation trends under these experimental conditions (Appendix A Fig. S2). In the presence of bromide, chloroform formation decreased by 82–95% compared to previous studies (Ackerson et al., 2018).

Iodo-THM formation and speciation changed substantially as iopamidol concentrations increased. The most predominant iodo-THM formed in the chlorinated SWs at different iopamidol concentrations was CHBrClI, accounting for 90% of the iodo-THMs formed (Fig. 3). CHBrClI formation increased as iopamidol concentration increased in both SWs, especially in BSW, and appears to be dependent on iopamidol and bromide concentrations. Also, $CHCl_2I$ increased with increasing iopamidol concentrations and pH (Fig. 3). BSW showed an increase of 1.2–2.3-fold in $CHCl_2I$ formation as iopamidol increased from 1.0 to 2.5 μmol/L and 1.2–3.0-fold from 2.5 to 5.0 μmol/L. $CHCl_2I$ formation in CSW exhibited a marginal increase from 1

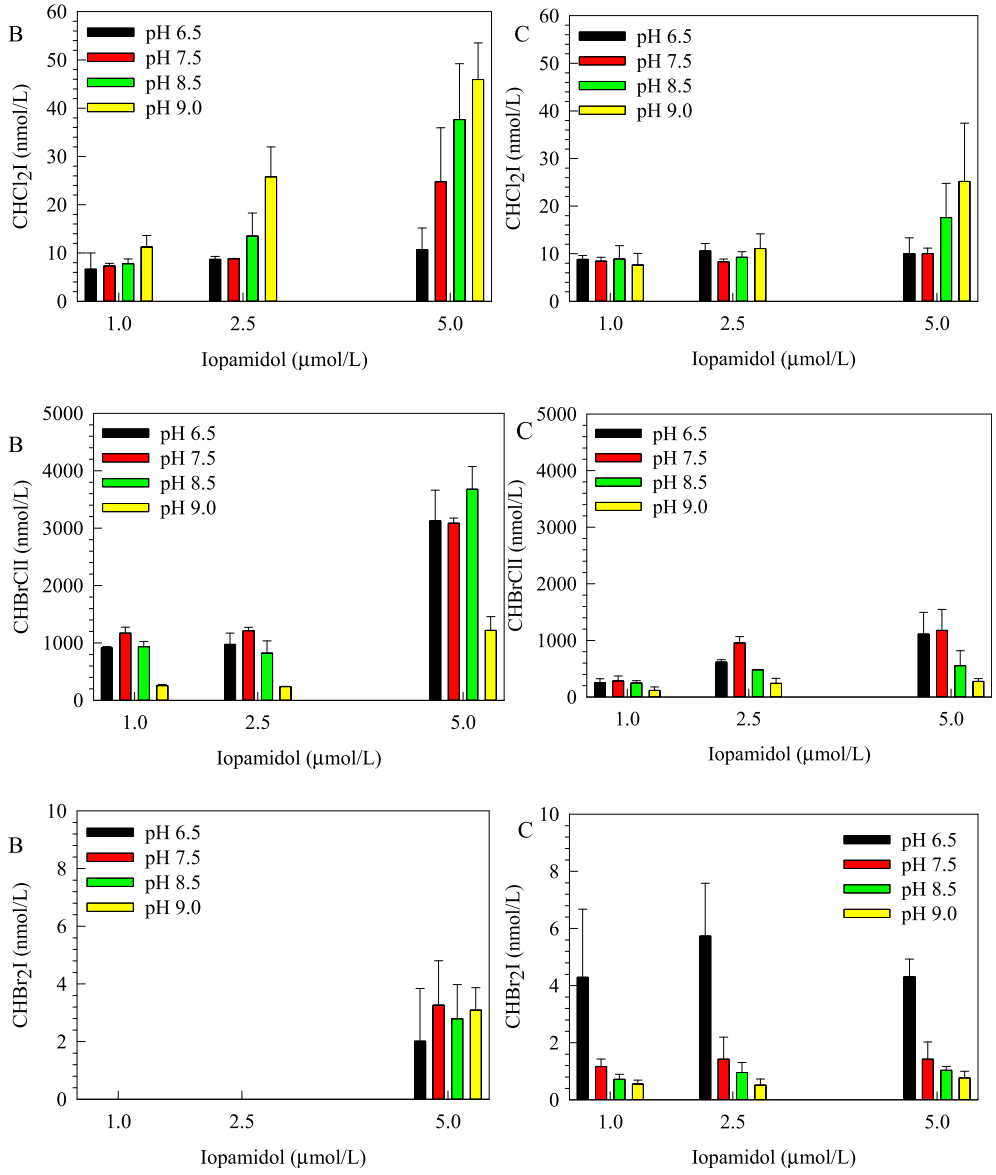


**Fig. 3 – Iodo-THM formation in chlorinated Barberton and Cleveland source waters as a function of iopamidol concentration and pH at 48 hr. $[Cl_2]_T$ = 100 μmol/L, [Iopamidol] = 1–5 μmol/L, $[Br^-]$ = 15 μmol/L, $[Buffer]_T$ = 4 mmol/L, Temp = 25°C, $DOC_{Barberton}$ = 4.47 mg/L-C, $DOC_{Cleveland}$ = 2.51 mg/L-C. Error bars represent 95% confidence interval for three replicates.**

to 2.5 μmol/L and increased approximately 2.5-fold when iopamidol concentrations increased from 2.5 to 5.0 μmol/L. The addition of $Br^-$ to the SWs at all iopamidol concentrations resulted in a 35%–90% decrease in $CHCl_2I$ formation (Ackerson et al., 2018). While $CHClI_2$ formation was observed, it was less than 5 nmol/L, regardless of pH, SW, or iopamidol concentration (Appendix A Fig. S2). $CHBr_2I$ was below detection limits at iopamidol concentrations of 1 and 2.5 μmol/L, but significant concentrations were detected at higher iopamidol concentrations in BSW (Fig. 3) while $CHBr_2I$ formation in CSW did not appear to vary significantly as a function of iopamidol concentration. Generally, most of the iodo-THMs increased with increasing iopamidol due to a greater potential for HOI formation (Duirk et al., 2011). Deiodination of iopamidol DBPs contributed to iodo-THM formation. DBAN formation was observed but showed little dependence on iopamidol concentration (Appendix A Fig. S3). The presence of $Br^-$ resulted in decreases in $CHCl_3$ and $CHCl_2I$ formation but favored CHBrClI formation.

Chlorinated HAAs also showed a significant shift in concentrations and speciation due to the presence of bromide. DCAA formation in BSW and CSW was in the range of 34–114 and 25–53 nmol/L, respectively at all iopamidol concentrations (Appendix A Fig. S4). Generally, DCAA concentrations decreased with increasing iopamidol concentration, but the decreases were not substantial. Almost equal concentrations of TCAA (37–139 nmol/L) were formed at 1.0 and 2.5 μmol/L iopamidol but decreased by 42%–57% at 5.0 μmol/L in BSW. In CSW, approximately equal formation of TCAA (16–26 nmol/L) was detected at 1.0 and 5.0 μmol/L but increased to 22–28 nmol/L at iopamidol concentration of 2.5 μmol/L (Appendix A Fig. S4). At all iopamidol concentrations, TCAA concentrations decreased by 60%–95% when the SWs were spiked with $Br^-$, compared to the same SWs without $Br^-$ (Ackerson et al., 2018).

About 15–28 nmol/L and 59–110 nmol/L of BAA and DBAA were formed, respectively, in BSW, whereas 5–13 nmol/L and 31–66 nmol/L were produced, respectively, in CSW (Appendix A Fig. S5). The highest concentrations of TBAA formed at all pH levels and at iopamidol concentration of 2.5 and 5.0 μmol/L, respectively in BSW (82–254 nmol/L) and CSW (25–77 nmol/L) except at pH 6.5 in BSW (Appendix A Fig. S5). The quantity of BCAA increased by 3%–36% from iopamidol concentration of 1.0–2.5 μmol/L and decreased by 31%–72% from 2.5 to 5.0 μmol/L in BSW (Appendix A Fig. S6). In CSW, BCAA increased by less than two-fold with increasing iopamidol concentration. Approximately the same amount of DBCAA (50–257 nmol/L) was formed in BSW at all pHs, while equal concentrations (36–40 nmol/L) were formed in CSW at lower pH at iopamidol concentrations of 2.5 and 5.0 μmol/L (Appendix A Fig. S6). The formation of BDCAA in BSW and CSW was respectively between 14 and 82 nmol/L and 2–21 nmol/L (Appendix A Fig. S6). Trace concentrations of iodo-HAAs (except DIAA) were detected in BSW at all iopamidol concentrations but were below the limit of quantification. Only BIAA was detected in CSW at iopamidol concentration of 5 μmol/L; the other iodo-HAA species were below the limit of detection. The presence of $Br^-$ appears to inhibit iodo-HAA formation in these SWs when iopamidol is the iodine source compared to studies without $Br^-$ (Ackerson et al., 2018).

### 2.3. Formation of TOX and DBPs at different bromide levels in the presence of NOM

Formation and speciation of TOX and DBPs were determined in both chlorinated BSW and CSW at $Br^-$ concentrations of 2, 15, and 30 μmol/L while maintaining iopamidol concentration (5 μmol/L) constant. The experiments were conducted for 48 hr to ensure adequate oxidant was present since high concentrations of bromide accelerate chlorine loss. TOI loss in BSW and CSW (Appendix A Fig. S7) was less than 30%, regardless of SW. TOI loss was approximately equal to TOI loss in the same SWs without $Br^-$, and inorganic iodine species were not detected as previously reported (Ackerson et al., 2018).

Substantial concentrations of TOBr formation were observed due to bromide oxidation by aqueous chlorine. Bromide oxidation results in the formation of HOBr, which less selectively than HOCl, reacts/incorporates into the NOM structure (Criquet et al., 2015), as well as iopamidol DBPs. TOBr formation in BSW and CSW increased with increasing $Br^-$ concentration and pH. In Appendix A Fig. S7, bromide was completely incorporated at low (2 μmol/L) and medium (15 μmol/L) $Br^-$ concentrations in BSW. However, 77–87% incorporation was observed at the high $Br^-$ (30 μmol/L) concentration in BSW and appeared to increase as function of pH. At a $Br^-$ concentration of 2 μmol/L in CSW, 100% of the added bromide was incorporated to form TOBr. At a $Br^-$ concentration of 15 μM in CSW, 76% and 82% bromide were incorporated at the end of 48 hr at pH 6.5 and 7.5 respectively, while approximately 100% incorporation was seen at pH 8.5 and 9.0. Less than 66% of 30 μmol/L $Br^-$ formed TOBr in CSW regardless of pH due to the low DOC concentration. At 48 hr, the amount of bromide detected at high bromide concentration ranged from 5.2 to 11.3 μmol/L in BSW and 2.2–11.0 μmol/L in CSW. Higher concentrations of bromide were detected at lower pH. All the bromide in BSW was accounted for in the sum of the TOBr and residual bromide concentrations; however, for CSW, only 80% was recovered and no bromate was detected. This mass balance discrepancy could be due in part to less adsorbable TOBr formation in CSW.

As bromide concentrations increased, TOCl concentrations decreased, because of increased initial chlorine demand and rapid reaction with $Br^-$ to form HOBr (Kumar and Margerum, 1987; Margerum and Hartz, 2002). Therefore, the limited residual chlorine, also in competition with other halogens, incorporated into NOM structure and iopamidol DBPs. TOCl decreased by 40%–48% and further by 12%–33% as $Br^-$ concentration increased from 2 to 15 and 30 μmol/L, respectively, with no discernible pH dependency (Appendix A Fig. S7). The higher concentrations of TOCl formed in BSW than CSW can be attributed to BSW having higher $SUVA_{254}$ (Appendix A Table S1).

All regulated THMs, as well as iodo-THMs, were detected regardless of the bromide concentration initially present. THM formation usually increased with increasing pH, as

observed in other studies (Hua and Reckhow, 2012, 2008). $CHCl_3$ decreased with increasing bromide concentrations (Appendix A Fig. S8). In CSW, $CHCl_3$ decreased by approximately 50% as $Br^-$ levels increased from 2.0 to 15 μmol/L and continued as bromide concentrations increased to 30 μmol/L. Also, $CHCl_3$ quantities at $Br^-$ concentration of 2 μmol/L dropped by 2–3 fold when compared with studies without $Br^-$ (Ackerson et al., 2018). In BSW, greater than a 90% drop in $CHCl_3$ concentration was observed when bromide increased from 2 to 30 μmol/L and there was an approximately 30% decrease from no $Br^-$ to 2 μmol/L $Br^-$. $CHBrCl_2$ and $CHBr_2Cl$ did not exhibit any discernible formation trends with $Br^-$ concentrations in both SWs (Appendix A Fig. S8). $CHBr_3$ showed substantial increases with increasing $Br^-$ concentrations, as well as pH, in BSW and CSW (Appendix A Fig. S9). Almost equal quantities of $CHBr_3$ were formed at low $Br^-$ concentration in both BSW and CSW. However, up to two orders of magnitude greater concentrations of $CHBr_3$ were detected in BSW at increasing $Br^-$ concentrations compared to CSW. At the highest bromide concentrations, more $CHBr_3$ formed than $CHCl_3$ at the lowest bromide concentrations (Ackerson et al., 2018). This could be due to HOBr incorporating better into reactive sites than aqueous chlorine (Westerhoff et al., 2004).

The iodo-THMs formed were mainly mixed halogenated species. The predominant iodo-THM was $CHCl_2I$ at low $Br^-$ dose (especially in BSW). $CHCl_2I$ levels decreased by 65%–87% from low to medium $Br^-$ concentration and 26%–86% from medium to high levels in BSW (Fig. 4). In CSW a decrease of 37%–80% was recorded as $Br^-$ concentrations increased from 2 to 30 μmol/L. CHBrClI was the most predominant iodo-THM as bromide concentrations increased in the SWs (Fig. 4). The formation of CHBrClI in BSW showed a substantial increase (12–37 times) as $Br^-$ increased from 2 to 15 μmol/L but reduced by 22%–62% at $Br^-$ dosage of 30 μmol/L at all pH levels. It appears that the increasing formation of $CHBr_3$ at higher $Br^-$ concentration suppressed the formation of CHBrClI, as well as

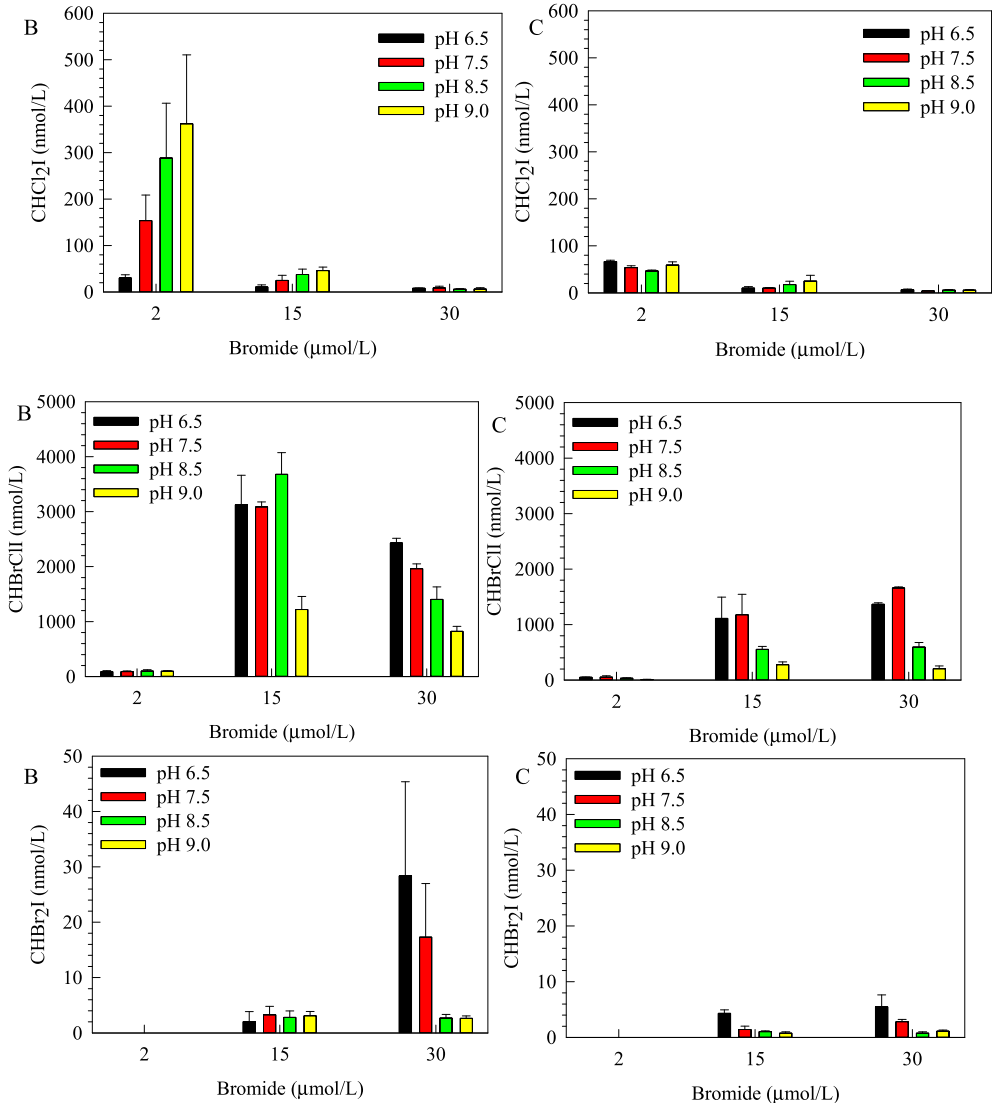


**Fig. 4 – Iodo-THM formation in chlorinated Barberton and Cleveland source waters as a function of bromide concentration and pH at 48 hr. $[Cl_2]_T$ = 100 μmol/L, [Iopamidol] = 5 μmol/L, $[Br^-]$ = 1–30 μmol/L, $[Buffer]_T$ = 4 mmol/L, Temp = 25°C, $DOC_{Barberton}$ = 4.47 mg/L-C, $DOC_{Cleveland}$ = 2.51 mg/L-C. Error bars represent 95% confidence interval of three replicates.**

other DBPs previously discussed. $CHClI_2$ was detected at all $Br^-$ concentrations in BSW but at medium and high concentration in CSW and was generally less than 10 nmol/L (Appendix A Fig. S9). $CHClI_2$ generally decreased as pH increased in BSW, while no discernible DBP formation pattern as a function of $Br^-$ concentration and pH was established for the CSW. Substantial quantities of $CHBr_2I$ were detected at medium and high $Br^-$ concentrations in the SWs (Fig. 4). $CHBr_2I$ increased with $Br^-$ concentrations but did not exhibit a discernible pH trend. $CHBr_2I$ was not detected at low $Br^-$ concentrations in both SWs. Relatively low quantities of $CHBrI_2$ were found in BSW (Appendix A Fig. S9) at medium and high concentrations of $Br^-$, but it was below the limit of quantitation in CSW. The only HAN identified in both chlorinated SWs was DBAN. DBAN increased with increasing $Br^-$ concentration but decreased with increasing pH in both BSW and CSW (Appendix A Fig. S10). However, DBAN was detected only at pH 6.5 and 7.5 at all levels of $Br^-$ in CSW.

DCAA and TCAA were the only two chloro-HAAs detected in both chlorinated SWs. As expected, DCAA and TCAA concentrations decreased as $Br^-$ concentrations increased from zero to 30 μmol/L (Appendix A Fig. S11). On the other hand, bromo-HAA formation increased with increasing bromide concentrations. Formation of BAA in CSW (2–22 nmol/L) was relatively low compared to BSW (7–67 nmol/L) at all pH (Appendix A Fig. S12). Also, DBAA formation increased with increasing $Br^-$ concentrations in both SWs (Appendix A Fig. S12). From low to medium $Br^-$ dosage, a two-fold and up to three-fold increase in DBAA concentrations was observed for BSW and CSW. Increasing bromide concentration from 15 to 30 μmol/L, observed DBAA formation increased but was not substantial for both SWs. At low $Br^-$ concentrations, TBAA formation in the SWs was 12–23 nmol/L (Appendix A Fig. S12). As the amount of $Br^-$ increased, TBAA formation was greater in BSW (up to 515 nmol/L) than CSW (up to 94 nmol/L). The higher increase in BSW could be attributed to the higher $SUVA_{254}$.

Under these experimental conditions, mixed bromo-chloro-HAAs species identified were BCAA, BDCAA, and DBCAA (Appendix A Fig. S13). Generally, BCAA decreased (20%–52%) from low to intermediate $Br^-$ concentration but increased by 2–7 times at high $Br^-$ concentration in BSW. Nevertheless, BCAA quantities increased by two-fold from low to medium and 6–61% from medium to high $Br^-$ concentrations in CSW. In addition, the formation of BDCAA in BSW and CSW was between 14 and 82 nmol/L and 2–21 nmol/L, respectively and, generally decreased with increasing $Br^-$concentrations. Further, the concentration of DBCAA formed in BSW and CSW were 15–258 nmol/L and 2–40 nmol/L, respectively. Generally, the highest DBCAA quantities in BSW and CSW occurred at $Br^-$ concentrations of 15 and 30 μmol/L, respectively.

Formation of iodo-HAAs was observed, but the concentrations were extremely low. While less than 10 nmol/L of iodo-HAAs – IAA, CIAA, BIAA, and DIAA – were formed in the SWs at the end of 48 hr, there were no discernible trends with respect to either bromide concentration or pH (Appendix A Fig. S14). Generally, the highest formation of each iodo-HAA species occurred at low $Br^-$ concentration except for BIAA quantities in BSW. CIAA was the predominant iodo-HAA in the SWs, but was not detected at all bromide concentrations in CSW. IAA and CIAA were observed at all bromide concentrations in BSW, but only at bromide concentration of 2 μM in CSW. Trace quantities of BIAA were detected in the chlorinated SWs containing iopamidol at different $Br^-$ concentrations. DIAA was only observed in BSW at low $Br^-$ concentration.

In effect, increasing $Br^-$ concentration shifted HAAs from chlorinated species to mixed halogenated species to fully brominated species. This agrees with other studies that investigated the impact of bromide on NOM reactions with chlorine (Cowman and Singer, 1996; Hua et al., 2006). In the presence of bromide, $Br^-$ outcompeted iopamidol and suppressed iodo-DBP formation, especially chloro-iodo-DBPs. This is likely due to the faster incorporation of $Br^-$ into reactive sites (Westerhoff et al., 2004) and the slow degradation of iopamidol (Wendel et al., 2014). This result is different from chlorination of the same SWs in the absence of $Br^-$, where higher concentrations of iodo-DBPs were observed (Ackerson et al., 2018). Except for DBAA, HAAs generally increased with decreasing pH. The inverse pH trend exhibited by these HAAs can be attributed to a general acid-catalyzed reaction (Hua and Reckhow, 2012).

### 2.4. *Distribution of TOX in source waters*

#### 2.4.1. *Varying iopamidol concentration*

At all concentrations of iopamidol in the SWs, bromo-chloro-iodo-THMs was the highest fraction (4%–52%) of TOI representing the known DBPs (Table 1). Less than 1% of the TOI accounted for chloro-iodo-THMs (i.e. $CHCl_2I$ and $CHClI_2$) and bromo-iodo-THMs (i.e. $CHBr_2I$ and $CHBrI_2$). Unknown TOI (UTOI) in BSW and CSW was the highest percentage (46%–97%) of TOI at all iopamidol concentrations. The high proportion of UTOI may be from iopamidol DBPs. UTOI decreased from pH 6.5 to 7.5 and then increased from pH 7.5 to 9.0. This observation may have resulted from the participation of both HOCl and $OCl^-$ in the degradation of iopamidol to form iopamidol DBPs (Wendel et al., 2014). In BSW, bromo-chloro-THMs represented the highest percentage (18%–27%) of TOCl representing the known DBPs at low and mid-range iopamidol concentrations, while bromo-chloro-iodo-THMs (CHBrClI) were the most predominant fraction (17%–38%) at high concentration (Appendix A Table S3). On the contrary, bromo-chloro-iodo-THMs dominated the fractions (1%–15%) of known DBPs in CSW at all iopamidol concentrations (Appendix A Table S3). UTOCl fractions were <60% in BSW, but >88% in CSW.

Bromo-chloro-THMs recorded the highest percentage (14%–18%) of TOBr of the known classes of DBPs at low and medium iopamidol concentrations, but bromo-chloro-iodo-THMs dominated (8%–25%) at high concentration in BSW, except at pH 9.0 (Appendix A Table S4). Other known classes of DBPs that formed significant proportions of TOBr in BSW were bromo-THMs ($CHBr_3$) (3%–16%) and bromo-HAAs (BAA, DBAA, and TBAA) (2%–11%). In CSW, the highest percentage of TOBr in the known DBP classes were bromo-chloro-iodo-THMs (1%–10%) and bromo-THMs (3%–6%) at low and high pH, respectively (Appendix A Table S4). The proportions of

**Table 1 – Proportions (%) of TOI in chlorinated Barberton and Cleveland source waters as a function of iopamidol concentration and pH.**

| Species | pH | Barberton | | | Cleveland | | |
|---|---|---|---|---|---|---|---|
| | | Iopamidol concentration (μmol/L) | | | Iopamidol concentration (μmol/L) | | |
| | | 1.0 | 2.5 | 5.0 | 1.0 | 2.5 | 5.0 |
| Chloro-iodo-THM | 6.5 | 0.47 | 0.26 | 0.18 | 0.53 | 0.23 | 0.09 |
| | 7.5 | 0.43 | 0.22 | 0.27 | 0.46 | 0.19 | 0.05 |
| | 8.5 | 0.43 | 0.28 | 0.34 | 0.49 | 0.19 | 0.08 |
| | 9.0 | 0.48 | 0.54 | 0.38 | 0.45 | 0.22 | 0.08 |
| Bromo-chloro-iodo-THM | 6.5 | 33.61 | 17.48 | 25.99 | 11.83 | 10.83 | 12.00 |
| | 7.5 | 52.17 | 23.64 | 26.46 | 14.14 | 19.83 | 16.17 |
| | 8.5 | 41.37 | 16.32 | 32.57 | 13.47 | 9.49 | 5.92 |
| | 9.0 | 10.52 | 4.70 | 9.92 | 6.73 | 4.64 | 2.51 |
| Bromo-iodo-THM | 6.5 | ND | ND | 0.02 | 0.21 | 0.10 | 0.05 |
| | 7.5 | ND | ND | 0.03 | 0.07 | 0.03 | 0.03 |
| | 8.5 | ND | ND | 0.03 | 0.04 | 0.02 | 0.01 |
| | 9.0 | ND | ND | 0.03 | 0.04 | 0.01 | 0.01 |
| UTOI | 6.5 | 65.92 | 82.26 | 73.80 | 87.43 | 88.84 | 87.86 |
| | 7.5 | 47.41 | 76.14 | 73.24 | 85.33 | 79.95 | 83.75 |
| | 8.5 | 58.21 | 83.40 | 67.05 | 85.99 | 90.30 | 94.00 |
| | 9.0 | 88.99 | 94.76 | 89.67 | 92.79 | 95.13 | 97.39 |

$[Cl_2]_T$ = 100 μmol/L, [Iopamidol] = 1–5 μmol/L, $[Br^-]$ = 15 μmol/L, $[Buffer]_T$ = 4 mmol/L, Temp = 25°C, $DOC_{Barberton}$ = 4.47 mg/L-C, $DOC_{Cleveland}$ = 2.51 mg/L-C. UTOI: Unknown TOI. ND: Not detected.

unknown TOBr (UTOBr) in CSW decreased with increasing amount of iopamidol, but the reductions were not substantial.

#### 2.4.2. *Varying bromide concentration*

Regardless of bromide concentration, the predominant fraction of TOI in these SWs were UTOI (>89%) (Appendix A Table S5), and, it generally decreased with $Br^-$ concentration. In both BSW and CSW, the highest fraction of known DBPs was chloro-iodo-THMs (0.3%–3.1%). However, as bromide concentrations increased, bromo-chloro-iodo-THMs formed the most predominant percentage of DBPs.

UTOCl was the predominant (41%–69%) TOCl percentage at low and medium $Br^-$ concentrations in BSW except at pH 8.5 at medium concentration (Appendix A Table S6). At high $Br^-$ concentration, the highest percentages of TOCl were bromo-chloro-THMs ($CHBr_2Cl$ and $CHBrCl_2$) (32%–37%) and UTOCl (33%–52%) at low and high pH, respectively. The highest percentage of TOCl in CSW (67%–93%), regardless of bromide concentration and pH, was UTOCl (Appendix A Table S6).

Generally, the predominant fractions of the DBP classes in BSW were bromo-chloro-THMs (30%–41%), bromo-chloro-iodo-THMs (20%–25%), and bromo-THMs (28%–56%) at low, medium (except at pH 9.0), and high $Br^-$ concentrations (Appendix A Table S6). In CSW, bromo-chloro-THMs recorded the greatest proportion (6%) of TOBr in the known classes of DBPs at low $Br^-$ concentration (Appendix A Table S7). However, bromo-chloro-iodo-THMs (9%–12%) and bromo-THMs (4%–8%) were the highest percentages of TOBr among the known DBPs at increasing $Br^-$ concentrations at low (pH 6.5 and 7.5) and high pH (8.5 and 9.0) respectively in CSW. An appreciable decrease in UTOBr with increasing $Br^-$ concentration was observed in BSW. Nonetheless, the proportion of UTOBr marginally decreased to approximately 79% at pH 6.5 and 7.5 but increased to approximately 89% at pH 8.5 and 9.0 as the concentrations of $Br^-$ increased in CSW.

## 3. Conclusions

This study investigated the inhibition of iodo-DBP formation in the presence of bromide when iopamidol is the iodinated DBP precursor. In the absence of NOM, the degradation of iopamidol in the presence of $Br^-$ and aqueous chlorine formed $CHCl_3$, $CHBrCl_2$, $CHBr_2Cl$, $CHBr_3$, CHBrClI, and TCAA as well as halogen specific TOX and iodate. In the presence of NOM, incorporation of bromine and chlorine into NOM increased the observed concentrations of TOBr and TOCl by approximately 5–61% and 2–50%, respectively. In addition, less than 30% TOI loss was observed under varying bromide and iopamidol concentrations. The presence of bromide substantially inhibited iodo-DBP formation, especially non-brominated iodo-DBPs. In the presence of $Br^-$, $CHCl_2I$ decreased by 35%–90%, regardless of iopamidol concentrations. At both 1 μmol/L iopamidol/15 μmol/L bromide and 2 μmol/L bromide/5 μmol/L iopamidol, significant quantities of highly genotoxic iodo-DBPs were formed. However, the presence of bromide may mitigate the formation of iodo-DBPs resulting at environmentally relevant conditions.

## Conflict of interest

The authors declare that they have no known competing financial interests or personal relationships that could have appeared to influence the work reported in this paper.

## Acknowledgments

This study was supported by the German Research Foundation (Deutsche Forschungsgemeinschaft, DFG, project number TE 533/4-1) and the National Science Foundation (NSF, project numbers NSF1124865 and NSF1124844).

## Appendix A. Supplementary data

Supplementary data to this article can be found online at https://doi.org/10.1016/j.jes.2019.10.007.

## REFERENCES


Ackerson, N.O.B., Machek, E.J., Killinger, A.H., Crafton, E.C., Kumkum, P., Liberatore, H.K., et al., 2018. Formation of DBPs and halogen-specific TOX in the presence of iopamidol and chlorinated oxidants. Chemosphere 202, 349–357.

Agus, E., Voutchkov, N., Sedlak, D.L., 2009. Disinfection by-products and their potential impact on the quality of water produced by desalination systems: A literature review. Desalination 237, 214–237.

Allen, J., Cuthbertson, A.A., Liberatore, H.K., Kimura, S.Y., Mantha, A., Edwards, M.A., et al., 2017. Showering in Flint, MI: Is there a DBP problem? J. .Environ. Sci. 58, 271–284.

APHA, AWWA, WEF, 2005. Standard Methods for the Examination of Water and Wastewater, 20 ed. American Public Health Association, Washington DC.

Arslan-Alaton, I., Olmez-Hanci, T., Korkmaz, G., Sahin, C., 2016. Removal of iopamidol, an iodinated X-ray contrast medium, by zero-valent aluminum-activated H2O2 and S2O82-. Chem. Eng. J. 318, 64–75.

Attene-Ramos, M., Wagner, E.D., Plewa, M.J., 2010. Comparative Human Cell Toxicogenomic Analysis of Monohaloacetic Acid Drinking Water Disinfection Byproducts. Environ. Sci. Technol. 44, 7206–7212.

Bichsel, Y., von Gunten, U., 1999. Oxidation of iodide and hypoiodous acid in the disinfection of natural waters. Environ. Sci. Technol. 33, 4040–4045.

Christiansen, C., 2005. X-ray contrast media - an overview. Toxicology 209, 185–187.

Christman, R.F., Norwood, D.L., Millington, D.S., Johnson, J.D., Stevens, A.A., 1983. Identity and yields of major halogenated products of aquatic fulvic-acid chlorination. Environ. Sci. Technol. 17, 625–628.

Cowman, G.A., Singer, P.C., 1996. Effect of bromide ion on haloacetic acid speciation resulting from chlorination and chloramination of aquatic humic substances. Environ. Sci. Technol. 30, 16–24.

Criquet, J., Allard, S., Salhi, E., Joll, C.A., Heitz, A., von Gunten, U., 2012. Iodate and Iodo-Trihalomethane Formation during Chlorination of Iodide-Containing Waters: Role of Bromide. Environ. Sci. Technol. 46, 7350–7357.

Criquet, J., Rodriguez, E.M., Allard, S., Wellauer, S., Salhi, E., Joll, C.A., et al., 2015. Reaction of bromine and chlorine with phenolic compounds and natural organic matter extracts - Electrophilic aromatic substitution and oxidation. Water Res. 85, 476–486.

Dad, A., Jeong, C.H., Pals, J.A., Wagner, E.D., Plewa, M.J., 2013. Pyruvate remediation of cell stress and genotoxicity induced by haloacetic acid drinking water disinfection by-products. Environ. Mol. Mutagen. 54, 629–637.

Doll, T.E., Frimmel, F.H., 2005. Photocatalytic degradation of carbamazepine, clofibric acid and iomeprol with P25 and Hombikat UV100 in the presence of natural organic matter (NOM) and other organic water constituents. Water Res. 39, 403–411.

Duan, X., He, X., Wang, D., Mezyk, S.P., Otto, S.C., Marfil-Vega, R., et al., 2016. Decomposition of Iodinated Pharmaceuticals by UV-254 nm-assisted Advanced Oxidation Processes. J. Hazard. Mater. 323, 489–499.

Duirk, S.E., Cherney, D.P., Tarr, J.C., Collette, T.W., 2006. Determining Active Oxidant Species Reacting with Organophosphate Pesticides in Chlorinated Drinking Water USEPA, pp. 1–69.

Duirk, S.E., Lindell, C., Cornelison, C.C., Kormos, J., Ternes, T.A., Attene-Ramos, M., et al., 2011. Formation of Toxic Iodinated Disinfection By-Products from Compounds Used in Medical Imaging. Environ. Sci. Technol. 45, 6845–6854.

Duirk, S.E., Valentine, R.L., 2007. Bromide oxidation and formation of dihaloacetic acids in chloraminated water. Environ. Sci. Technol. 41, 7047–7053.

Heeb, M.B., Criquet, J., Zimmermann-Steffens, S.G., von Gunten, U., 2014. Oxidative treatment of bromide-containing waters: Formation of bromine and its reactions with inorganic and organic compounds - A critical review. Water Res. 48, 15–42.

Hu, J., Song, H., Karanfil, T., 2010. Comparative Analysis of Halonitromethane and Trihalomethane Formation and Speciation in Drinking Water: The Effects of Disinfectants, pH, Bromide, and Nitrite. Environ. Sci. Technol. 44, 794–799.

Hua, G., Reckhow, D.A., 2008. DBP formation during chlorination and chloramination: Effect of reaction time, pH, dosage, and temperature. J. Am. Water Works Assoc. 100, 82–95.

Hua, G., Reckhow, D.A., 2012. Effect of alkaline pH on the stability of halogenated DBPs. J. Am. Water Works Assoc. 104, 49–50.

Hua, G., Reckhow, D.A., Abusallout, I., 2015. Correlation between SUVA and DBP formation during chlorination and chloramination of NOM fractions from different sources. Chemosphere 130, 82–89.

Hua, G.H., Reckhow, D.A., Kim, J., 2006. Effect of bromide and iodide ions on the formation and speciation of disinfection byproducts during chlorination. Environ. Sci. Technol. 40, 3050–3056.

Krause, W., Schneider, P.W., 2002. Optical, ultrasound, X-ray and radiopharmaceutical imaging. In: Merbach, A.E., Toth, E. (Eds.), The Chemistry of Contrast Agents in Medical Magnetic Resonance Imaging. Wiley, New York, pp. 107–150.

Kumar, K., Margerum, D.W., 1987. Kinetics and mechanism of general-acid-assisted oxidation of bromide by hypochlorite and hypochlorous acid. Inorg. Chem. 26, 2706–2711.

Margerum, D.W., Hartz, K.E.H., 2002. Role of halogen(I) cation-transfer mechanisms in water chlorination in the presence of bromide ion. J. Environ. Monit. 4, 20–26.

Matsushita, T., Kobayashi, N., Hashizuka, M., Sakuma, H., Kondo, T., Matsui, Y., et al., 2015. Changes in mutagenicity and acute toxicity of solutions of iodinated X-ray contrast media during chlorination. Chemosphere 135, 101–107.

Nagy, J.C., Kumar, K., Margerum, D.W., 1988. Non-metal redox kinetics - oxidation of iodide by hypochlorous acid and by nitrogen trichloride measured by the pulsed-accelerated-flow method. Inorg. Chem. 27, 2773–2780.

Pals, J.A., Attene-Ramos, M., Xia, M., Wagner, E.D., Plewa, M.J., 2013. Human cell toxicogenomic analysis links reactive oxygen species to the toxicity of monohaloacetic acid drinking water disinfection byproducts. Environ. Sci. Technol. 47, 12514–12523.

Plewa, M.J., Simmons, J.E., Richardson, S.D., Wagner, E.D., 2010. Mammalian Cell Cytotoxicity and Genotoxicity of the Haloacetic Acids, A Major Class of Drinking Water Disinfection By-Products. Environ. Mol. Mutagen. 51, 871–878.

Plewa, M.J., Wagner, E.D., Richardson, S.D., Thruston, A.D., Woo, Y.T., McKague, A.B., 2004. Chemical and biological characterization of newly discovered lodoacid drinking water disinfection byproducts. Environ. Sci. Technol. 38, 4713–4722.

Postigo, C., DeMarini, D.M., Armstrong, M.D., Liberatore, H.K., Lamann, K., Kimura, S.Y., et al., 2018. Chlorination of Source Water Containing Iodinated X-ray Contrast Media: Mutagenicity and Identification of New Iodinated Disinfection Byproducts. Environ. Sci. Technol. 52, 13047–13056.

Rabai, G., Nagy, Z.V., Beck, M.T., 1987. Quantitative description of the oscillatory behavior of the iodate-sulfite-thiourea system in CSTR. React. Kinet. Catal. Lett. 33, 23–29.
Richardson, S.D., Fasano, F., Ellington, J.J., Crumley, F.G., Buettner, K.M., Evans, J.J., et al., 2008. Occurrence and mammalian cell toxicity of iodinated disinfection byproducts in drinking water. Environ. Sci. Technol. 42, 8330–8338.
Seitz, W., Weber, W.H., Jiang, J.-Q., Lloyd, B.J., Maier, M., Maier, D., et al., 2006. Monitoring of iodinated X-ray contrast media in surface water. Chemosphere 64, 1318–1324.
Ternes, T.A., Hirsch, R., 2000. Occurrence and behavior of X-ray contrast media in sewage facilities and the aquatic environment. Environ. Sci. Technol. 34, 2741–2748.
Tian, F.-X., Xu, B., Lin, Y.-L., Hu, C.-Y., Zhang, T.-Y., Xia, S.-J., et al., 2017. Chlor(am)ination of iopamidol: kinetics, pathways and disinfection by-products formation. Chemosphere 184, 489–497.
Troy, R.C., Kelley, M.D., Nagy, J.C., Margerum, D.W., 1991. Nonmetal redox kinetics - iodine monobromide reaction with iodide-ion and the hydrolysis of IBr. Inorg. Chem. 30, 4838–4845.
Wagner, E.D., Plewa, M.J., 2017. CHO cell cytotoxicity and genotoxicity analyses of disinfection by-products: An updated review. J. Environ. Sci. 58, 64–76.
Watanabe, Y., Leu Tho, B., Pham Van, D., Prudente, M., Aguja, S., Phay, N., et al., 2016. Ubiquitous Detection of Artificial Sweeteners and Iodinated X-ray Contrast Media in Aquatic Environmental and Wastewater Treatment Plant Samples from Vietnam, The Philippines, and Myanmar. Arch. Environ. Contam. Toxicol. 70, 671–681.
Wei, X., Wang, S., Zheng, W., Wang, X., Liu, X., Jiang, S., et al., 2013. Drinking Water Disinfection Byproduct Iodoacetic Acid Induces Tumorigenic Transformation of NIH3T3 Cells. Environ. Sci. Technol. 47, 5913–5920.
Wendel, F.M., Eversloh, C.L., Machek, E.J., Duirk, S.E., Plewa, M.J., Richardson, S.D., et al., 2014. Transformation of Iopamidol during Chlorination. Environ. Sci. Technol. 48, 12689–12697.
Westerhoff, P., Chao, P., Mash, H., 2004. Reactivity of natural organic matter with aqueous chlorine and bromine. Water Res. 38, 1502–1513.
Ye, T., Xu, B., Wang, Z., Zhang, T.-Y., Hu, C.-Y., Lin, L., et al., 2014. Comparison of iodinated trihalomethanes formation during aqueous chlor(am)ination of different iodinated X-ray contrast media compounds in the presence of natural organic matter. Water Res. 66, 390–398.
Zhao, C., Arroyo-Mora, L.E., DeCaprio, A.P., Sharma, V.K., Dionysiou, D.D., O'Shea, K.E., 2014. Reductive and oxidative degradation of iopamidol, iodinated X-ray contrast media, by Fe(III)-oxalate under UV and visible light treatment. Water Res. 67, 144–153.